



# Graphene oxide–silica composite coating hollow fiber solid phase microextraction online coupled with inductively coupled plasma mass spectrometry for the determination of trace heavy metals in environmental water samples

Shaowei Su, Beibei Chen, Man He, Bin Hu\*

Key Laboratory of Analytical Chemistry for Biology and Medicine (Ministry of Education), Department of Chemistry, Wuhan University, Wuhan 430072, PR China

## ARTICLE INFO

### Article history:

Received 28 November 2013

Received in revised form

26 January 2014

Accepted 28 January 2014

Available online 31 January 2014

### Keywords:

Graphene oxide–silica (GO–silica) composite

Hollow fiber solid phase microextraction

Inductively coupled plasma mass spectrometry

Trace metals

Environmental water samples

## ABSTRACT

In this work, a novel graphene oxide–silica (GO–silica) composite coating was prepared for hollow fiber solid phase microextraction (HF–SPME) of trace Mn, Co, Ni, Cu, Cd and Pb followed by on-line inductively coupled plasma mass spectrometry (ICP–MS) detection. The structure of the prepared graphene oxide and GO–silica composite was studied and elucidated by atomic force microscopy (AFM), transmission electron microscopy (TEM), Fourier transform infrared spectroscopy (FT–IR) and X-ray photoelectron spectroscopy (XPS). The GO–silica composite coated hollow fiber was characterized by scanning electron microscope (SEM), and the results show that the GO–silica composite coating possessed a homogeneous and wrinkled structure. Various experimental parameters affecting the extraction of the target metal ions by GO–silica composite coated HF–SPME have been investigated carefully. Under the optimum conditions, the limits of detection (LODs,  $3\sigma$ ) for Mn, Co, Ni, Cu, Cd and Pb were 7.5, 0.39, 20, 23, 6.7 and 28  $\text{ng L}^{-1}$  and the relative standard deviations (RSDs,  $C_{\text{Mn, Co, Cd}}=0.05 \mu\text{g L}^{-1}$ ,  $C_{\text{Ni, Cu, Pb}}=0.2 \mu\text{g L}^{-1}$ ,  $n=7$ ) were 7.2, 7.0, 5.6, 7.3, 7.8 and 4.6%, respectively. The accuracy of the proposed method was validated by the analysis of Certified Reference Material of GSBZ 50009–88 environmental water and the determined values were in a good agreement with the certified values. The proposed method has been successfully applied for the determination of trace metals in real environmental water samples with recoveries ranging from 85 to 119%.

© 2014 Elsevier B.V. All rights reserved.

## 1. Introduction

Heavy metals, which have been widely used in industry of plating, steel, electronics and metallurgy and so on, are inevitably discharged into the environmental waters. They are non-biodegradable and can enter into human body through food chain, thus cause various damages to human's health even if in low dose [1,2]. Therefore, it is urgent to develop a rapid, sensitive and reliable monitoring technique for heavy metals in the environmental waters. Inductively coupled plasma mass spectrometry (ICP–MS) is considered to be one of the most appropriate techniques for trace and ultra-trace elements' analysis because of its low limits of detection and isotopes capability. However, when the conventional ICP–MS was employed for real-world sample analysis, it still suffered from the mass spectroscopic interference and matrix effects [3]. Although the spectroscopic interference in

ICP–MS can be minimized by using high-resolution (HR) ICP–MS and collision/reaction cell (CRC) ICP–MS [4], these techniques are rarely used in routine analysis due to the high cost and complicated instruments, and what is more, they still suffer from matrix effects. Therefore, a sample pretreatment step, which can separate the analytes from the matrix and preconcentrate them before their measurement, is often mandatory [5].

Among various sample pretreatment techniques [5–8], in-tube solid phase microextraction (in-tube SPME), also called capillary microextraction (CME), has the advantages of low cost, simple operation, fast speed, high selectivity, low sample/reagent consumption as well as easy-to-automate and has been widely used for analysis of trace organic and inorganic analytes by on-line coupling with different detection instrumentations [5,9–13]. The extraction principle of in-tube SPME is based on the distribution equilibrium of target analytes between the sample and the coating material. Thus, the coating material plays a fundamentally important role in in-tube SPME which determines its selectivity and extraction efficiency. Up to now, besides the conventional organic poly(dimethyl siloxane) (PDMS) and poly(ethylene glycol) (PEG)

\* Corresponding author. Tel.: +86 27 68752162; fax: +86 27 68754067.  
E-mail address: [binhu@whu.edu.cn](mailto:binhu@whu.edu.cn) (B. Hu).

coatings [14], a large number of new in-tube SPME coatings have been increasingly developed, such as polypyrrole (PPY) [15], human low-density lipoprotein (LDL) [16], single-walled carbon nanotubes [17], chitosan [18], alumina [5] and silica modified coating [9]. However, the amount of the coatings on the inner surface of the fused-silica capillary is limited, which leads to a relatively low adsorption capacity of in-tube SPME. It has been demonstrated that the use of newly developed hollow fiber supported in-tube SPME (called in-tube hollow fiber solid phase microextraction, in tube HF-SPME) was one of the simplest ways to solve this problem, due to its high porosity [19,20]. Chen et al. [19] prepared a new hollow fiber coating by mixing partially sulfonated poly(styrene) (PSP) with mixed-sol of 3-mercaptopropyltrimethoxysilane (MPTS) and *N*-(2-aminoethyl)-3-aminopropyltrimethoxysilane (AAPTS) and developed a novel method based on in-tube HF-SPME on-line coupled with ion pair reversed phase-high performance liquid chromatography (HPLC)–ICP-MS for arsenic speciation. Compared with fused-silica capillary supported in tube SPME, higher extraction efficiency was obtained by HF supported in-tube SPME.

Since discovered in 2004 [21], graphene, a new two-dimensional material comprising a single layer of  $sp^2$ -hybridized carbon atoms [22], has become one of the hottest research topics and gained much attention in material sciences due to its various unique properties [23–25]. It was reported that graphene possesses a high theoretical specific surface area ( $2630 \text{ m}^2/\text{g}$ ) [23], suggesting a high sorption capacity. In addition, due to its large delocalized  $\pi$ -electron system, graphene can form a strong  $\pi$ - $\pi$  stacking interaction with the benzene ring [26]. These unique properties make graphene superior for the adsorption of benzenoid compounds [27–31]. However, the research about graphene as an adsorbent for heavy metals is scarce [32,33], owing to the lack of functional groups on its surface for effective binding with metal ions.

Graphene oxide (GO), a precursor to graphene after reduction, consists of a hexagonal carbon network bearing hydroxyl and epoxide functional groups on its “basal” plane, whereas the edges are mostly decorated by carboxyl and carbonyl groups [34,35]. These oxygen-containing functional groups can bind with metal ions, especially the multivalent metal ions, through both electrostatic and coordinate approaches. It can be estimated that GO is an ideal adsorbent for metal ions. Recently, the utilization of GO as a sorbent for the removal of heavy metal ions from water has been reported [36,37]. Yang et al. [36] found that the adsorption capacity of Cu(II) on GO was 10 times higher than that of Cu(II) on active carbon. Wang et al. [37] prepared a few-layered GO (FGO) and found that the maximum adsorption capacities of Pb(II) ion on FGO were higher than any currently reported materials. However, to the best of our knowledge, there were no reports on the use of GO as the adsorbent for the separation/preconcentration of metal ions. The possible reason was that the GO was highly hydrophilic due to the oxygen-containing functional groups in its structure and could be easily lost during extraction. Therefore, the successful application of GO as an adsorbent for trace metal analysis is highly dependent on the breakthroughs in improvement of its stability in aqueous solution.

The purpose of this work was to prepare GO–silica composite coating and develop a novel method of GO–silica composite coated HF-SPME on-line coupled to ICP-MS for the determination of trace metals in environmental waters. GO–silica composite was prepared with the addition of silica to enhance the coating stability. In another aspect, hollow fiber supported in-tube SPME instead of capillary supported in-tube SPME was employed in order to obtain high adsorption capacity due to the porosity of hollow fiber. The adsorption behaviors of various metal ions, including  $\text{Mn}^{2+}$ ,  $\text{Co}^{2+}$ ,  $\text{Ni}^{2+}$ ,  $\text{Cu}^{2+}$ ,  $\text{Cd}^{2+}$  and  $\text{Pb}^{2+}$  on the GO–silica composite coated HF,

were examined, and the optimal experimental conditions were established. The developed method was validated by the determination of trace metals in the environmental water samples.

## 2. Experimental

### 2.1. Instrumentations

An Agilent 7500a ICP-MS (Agilent, Tokyo, Japan) with a Babington nebulizer was applied and the optimal operating conditions are summarized in Table 1. The pH values were controlled by a Mettler Toledo 320-S pH meter (Mettler Toledo Instruments Co. Ltd., Shanghai, China) supplied with a combined electrode (LE438). An IFIS-C flow injection system (Ruimai Tech. Co. Ltd., Xi'an, China) was used for on-line coupling HF-SPME with ICP-MS. Polypropylene hollow fiber ( $600 \mu\text{m}$  i.d.  $\times$   $800 \mu\text{m}$  o.d., pore size:  $0.2 \mu\text{m}$ ) was obtained from Membrana (Wuppertal, Germany). PTFE tubing with  $0.5 \text{ mm}$  i.d. was used for all connections. These connections were kept as short as possible to minimize the dead volume.

### 2.2. Standard solutions and reagents

The stock standard solutions ( $1.000 \text{ g L}^{-1}$ ) of Cd, Co, Mn, Ni, Pb and Cu were prepared by dissolving appropriate amounts of Cd ( $\text{NO}_3)_2$ ,  $\text{Co}(\text{NO}_3)_2 \cdot 6\text{H}_2\text{O}$ ,  $\text{MnSO}_4$ ,  $\text{NiSO}_4 \cdot (\text{NH}_4)_2\text{SO}_4 \cdot 6\text{H}_2\text{O}$ ,  $\text{Pb}(\text{NO}_3)_2$  and  $\text{CuSO}_4 \cdot 5\text{H}_2\text{O}$  (all of analytical grade, The First Reagent Factory, Shanghai, China) in 1% (v/v) diluted  $\text{HNO}_3$ , respectively. Working solutions were prepared daily by appropriate dilutions of their stock solutions. Graphite powder (325 mesh, 99.9995%) was obtained from Alfa Aesar (MA, USA).  $\text{P}_2\text{O}_5$ ,  $\text{K}_2\text{S}_2\text{O}_8$ ,  $\text{H}_2\text{O}_2$ ,  $\text{KMnO}_4$ ,  $\text{HCl}$  and  $\text{H}_2\text{SO}_4$  were purchased from Sinopharm Chemistry Reagent Co. Ltd, China (Shanghai, China). Tetramethoxysilane (TMOS) was purchased from Organic Silicon Material Company of Wuhan University (Wuhan, China). High purity water ( $18.2 \text{ M}\Omega \text{ cm}$ ) obtained from Milli-Q Element system (Millipore, Molsheim, France) was used throughout this work. All reagents were of analytical grade unless otherwise specified. Plastic and glass containers and all other laboratory materials that could come into contact with samples and standards were stored in 20% (v/v) nitric acid over 24 h and rinsed with high purity water prior to use.

### 2.3. Synthesis and characterization of graphene oxide, graphene oxide–silica composite and silica coated hollow fiber

Graphite oxide was synthesized according to the modified Hummers' method [38,39]. Briefly, 3 g of graphite powder was added into a 25 mL 3-necked round-bottom flask containing 12 mL of concentrated  $\text{H}_2\text{SO}_4$ , 2.5 g of  $\text{K}_2\text{S}_2\text{O}_8$  and 2.5 g of  $\text{P}_2\text{O}_5$ , and the

**Table 1**  
Operating conditions of ICP-MS.

ICP-MS plasma	parameters
Rf power	1250 W
Plasma gas (Ar) flow rate	$14 \text{ L min}^{-1}$
Auxiliary gas (Ar) flow rate	$0.88 \text{ L min}^{-1}$
Carrier gas (Ar) flow rate	$1.08 \text{ L min}^{-1}$
Sampling depth	7.0 mm
Sampler/skimmer diameter orifice	Nickel 1.0 mm/0.4 mm
Time-resolved data acquisition	
Scanning mode	Peak-hopping
Dwell time	50 ms
Integration mode	Peak area
Points per spectral peak	1
Isotopes	$^{55}\text{Mn}$ , $^{59}\text{Co}$ , $^{60}\text{Ni}$ , $^{63}\text{Cu}$ , $^{111}\text{Cd}$ , $^{208}\text{Pb}$

mixture was kept at 80 °C for 4.5 h. After that, the mixture was diluted with 1 L of high purity water, filtrated, washed with water and dried at 40 °C. Then, the pretreated oxidized graphite was dispersed in 120 mL of concentrated H<sub>2</sub>SO<sub>4</sub> in a 3-necked round-bottom flask under stirring, and the 3-necked round-bottom flask was placed in an ice bath. 15 g of KMnO<sub>4</sub> was added slowly into the 3-necked round-bottom flask with temperature strictly controlled below 10 °C. Afterwards, the mixture was allowed to react at 35 °C for 7 days. Then, 250 mL of high purity water was added, and the mixture was kept at 98 °C for 2 h. After the temperature was reduced to 60 °C, 15 mL of H<sub>2</sub>O<sub>2</sub> (30%, v/v) was added and the mixture was further stirred for 2 h. The above mixture was centrifuged to collect the graphite oxide and the collected graphite oxide was washed with 10% (v/v) HCl solution for five times, and then washed with high purity water until the pH of the supernatant was neutral. After that, the graphite oxide was dried at room temperature.

Hollow fibers were cut into segments with a uniform length of 20 cm. The HF segments were sonicated for 2 min in acetone to remove the contaminants in the fiber, and dried prior to use.

For preparation of graphene oxide–silica composite coated hollow fiber, 50 mg of graphite oxide was dissolved in 5 mL of mixture solvent of high purity water and ethanol ( $V_{\text{water}}:V_{\text{ethanol}}=3:2$ ) and the mixture was sonicated for 1 h to exfoliate graphite oxide to GO. After 50 μL of 1 mol L<sup>-1</sup> HCl and 400 μL of TMOS were thoroughly mixed with the GO dispersion mentioned above, the mixture was stirred at ambient temperature for 1 h, allowing for the complete hydrolysis of TMOS to form homogeneous GO–silica sol. Then, 1 mL GO–silica sol was withdrawn in a syringe, and the GO–silica sol was pumped into the HF through a syringe pump with a flow rate of 0.1 mL min<sup>-1</sup>. The GO–silica sol was maintained in HF for 1 h to fully evaporate the solvent. The process was repeated for three times. Afterwards, the GO–silica composite coated hollow fiber was placed in an oven at 60 °C for 8 h to age the coating. After preparation, each end (2–3 cm) of the hollow fiber having large voids was cut off, and 15 cm long GO–silica composite coated hollow fibers were used for the extraction.

For comparison, the silica coated hollow fiber was also prepared according to the procedure described above, except that silica sol without graphene oxide involved was used to coat the HF.

For characterization of GO by transmission electron microscope (TEM), a drop of GO dispersion was placed on a carbon-coated copper grid, dried at room temperature, and then the TEM image of GO was performed on a JEM-2100 (HR) electron microscope (Tokyo, Japan). GO dispersion was drop-casted onto a fresh mica wafer and dried under room temperature, and the atomic force microscopy (AFM) image was taken in tapping mode on a Digital Instruments Nanoscope IV Multi-Mode scanning probe microscope (Veeco, USA). GO and GO–silica composite was synthesized in the container, placed in an oven at 60 °C for 8 h and employed for FT-IR and XPS characterization. IR spectra were obtained by a 170SX Fourier transform infrared (FT-IR) spectrometer (NICOLET, USA). The X-ray photoelectron spectra (XPS) were obtained on a KRATOS XSAM800 X-ray photoelectron spectrometer with Mg K $\alpha$  X-ray radiation as the X-ray source excitation. The hollow fiber and GO–silica composite coated hollow fiber were cut lengthwise for SEM characterization of their inner surface. The scanning electron micrograph (SEM) of the composite coating was obtained using an X-650 scanning electron microscope (Hitachi, Tokyo, Japan) at an acceleration voltage of 25 kV.

#### 2.4. On-line hollow fiber solid phase microextraction-ICP-MS system

The on-line HF-SPME-ICP-MS system employed in this work was similar to that described previously [5]. Briefly, a 15 cm GO–silica composite coated HF, connected to the flow injection with

a PTFE tubing (i.d. 0.5 mm), was used as the adsorption column to extract the target metal ions. When the sample solution was passed through the system with the aid of the flow injection, the target metal ions were adsorbed by the GO–silica composite coating. The retained target metal ions on the GO–silica composite coated HF were eluted with 100 μL of HNO<sub>3</sub> for on-line ICP-MS detection.

#### 2.5. Sample preparation

Three water samples of well water (Xianning, China), lake water (East Lake, Wuhan, China) and pond water (Wuhan University, Wuhan, China) were collected and filtered through the 0.45 μm membrane filter (Tianjing Jinteng Instrument Factory, Tianjin, China), then acidified to pH of about 1 with concentrated HNO<sub>3</sub> prior to storage. The pH value of the sample was adjusted to 5 with 0.1 mol L<sup>-1</sup> HNO<sub>3</sub> and NH<sub>3</sub>·H<sub>2</sub>O prior to extraction.

For analysis of GSBZ 50009-88 environmental water (Institute for Reference Materials of SEPA, Beijing, China), the ampoule was broken carefully at the neck and 10 mL of the sample was pipetted into 250 mL volumetric flask and diluted to the calibrate using high purity water according to the manual. The sample was further diluted and adjusted to pH 5 for subsequent analysis.

The blank was also prepared by the same procedure described above without adding analytes.

### 3. Results and discussion

#### 3.1. Characterization of graphene oxide and graphene oxide–silica coating

The structure and morphology of the prepared GO were characterized by atomic force microscopy (AFM) and transmission electron microscopy (TEM). From the AFM image shown in Fig. 1a, it can be seen that the thickness of the GO was in the range 0.5–1.5 nm, suggesting that the GO be completely exfoliated to single layer or a few layers. Fig. 1b is the TEM image of prepared GO. As can be seen, the GO showed a thin and lamellar structure, also indicating that a single layer or a few layers graphene oxides were formed.

To ascertain the decoration of GO with silica in GO–silica composite, FT-IR spectra were obtained from GO, GO–silica and silica. From the FT-IR spectra shown in Fig. 2, it can be seen that a characteristic feature of GO–silica when compared with silica is a C=O bond around 1735 cm<sup>-1</sup> and a C–O bond around 1384 cm<sup>-1</sup> [40], which are also visible in the GO spectra. This indicated that GO–silica composite was successfully prepared.

XPS was also employed to characterize the prepared GO and GO–silica composite, and the C 1s XPS spectra are shown in Fig. 3. From Fig. 3a, four Gaussian peaks with binding energies of 283.8 (C–C), 285.5 (C–O), 286.6 (C=O), and 287.1 eV (O=C–O) [41] were observed, and the ratio of carbon to oxygen (C/O) is ca. 2.34, indicating a high oxidation of the prepared GO. From the C 1s XPS spectra of GO–silica composite shown in Fig. 3b, it can be seen that four Gaussian peaks corresponding to C–C, C–O, C=O, and O=C–O existed as well. However, compared with Fig. 3a, the C 1s of O=C–O peak was decreased to 282.0 eV, probably because of the formation of O=C–O–Si bonds in GO–silica composite. The above results demonstrated a successful preparation of GO–silica composite with abundant oxygen-containing groups, which are expected to form strong surface complexes with metal ions.

Fig. 4 shows the SEM images of hollow fiber and GO–silica composite coated hollow fiber. From Fig. 4a ( $\times 5000$ ), it can be seen that the surface of the hollow fiber possessed a porous structure, which will benefit for the increase of the coating

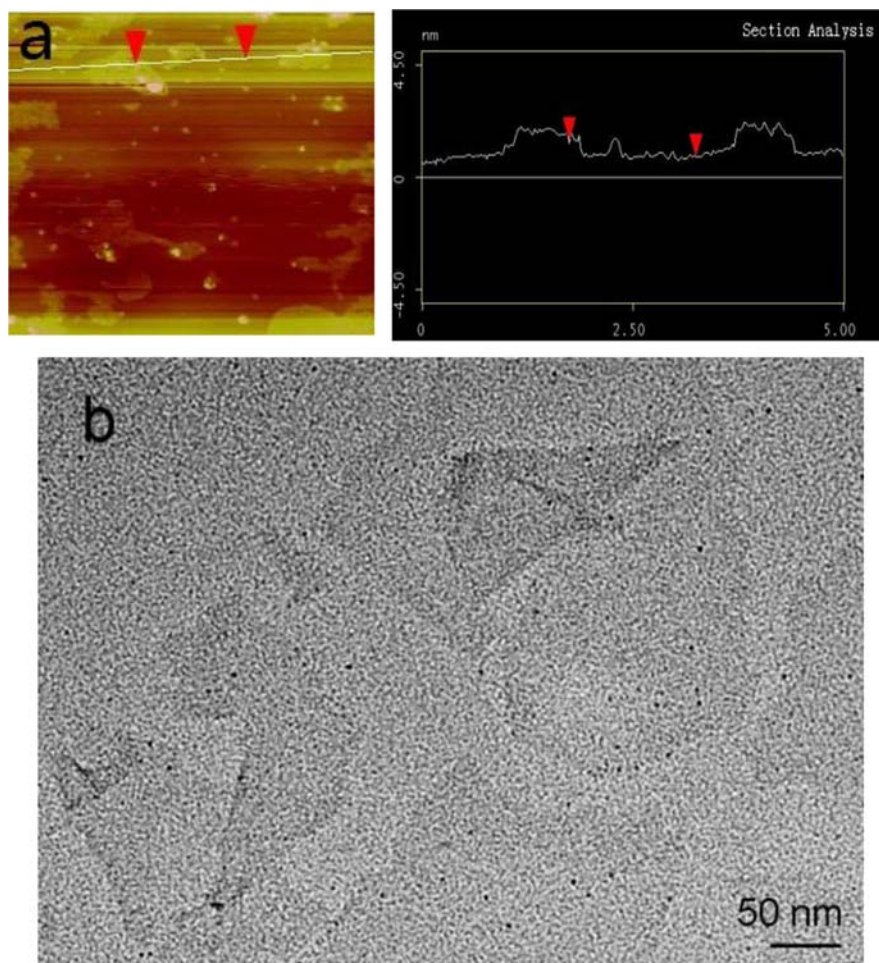


Fig. 1. AFM image of GO (a) and TEM image of GO (b).

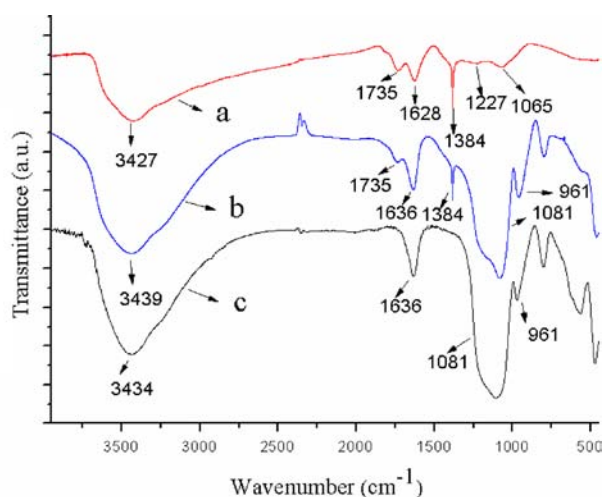


Fig. 2. FT-IR spectra of GO (a), GO-silica composite (b), and silica (c).

amount of GO-silica composite on the inner surface of the hollow fiber and the improvement of coating stability. Fig. 4b ( $\times 800$ ) shows that the GO-silica composite coating possessed a homogeneous and wrinkled structure. It indicated that the GO-silica composite was coated on the inner surface of the hollow fiber evenly, and the wrinkled structure of the coating could increase the surface area, as well as the adsorption capacity. From the enlarged SEM image of GO-silica composite coating in Fig. 4c

( $\times 1600$ ) and 4d ( $\times 6000$ ), it can be seen that GO sheets were homogeneously incorporated with the silica and interlocked together to form a compact film, indicating that the coating would be mechanically stable.

### 3.2. The optimization of hollow fiber solid phase microextraction procedure, effect of pH

pH value plays an important role with respect to the adsorption of different metal ions on GO-silica composite coated HF. An appropriate pH can not only improve the adsorption efficiency, but also depress the interference of coexisting ions. So, the effect of sample pH in the range of 2–9 on the adsorption percentages of target metal ions on the GO-silica composite coated HF was examined, and the results are shown in Fig. 5a. As can be seen, the adsorption percentage of all the target metal ions was increased rapidly with the increase of sample pH from 2 to 3, and quantitative adsorption was achieved when the sample pH was higher than 4. To ascertain the function of GO in GO-silica composite coating, the effect of sample pH on the adsorption of target metal ions by silica coated HF was also investigated and the results are shown in Fig. 5b. As can be seen, compared with the GO-silica composite coated HF, silica coated HF exhibited a totally different adsorption behavior towards the target metal ions. The adsorption percentage of the target metal ions on silica coated HF was lower than 20% when the sample pH was lower than 4. Although Pb, Cu and Cd could be quantitatively adsorbed at the sample pH higher than 8, the quantitative adsorption for other

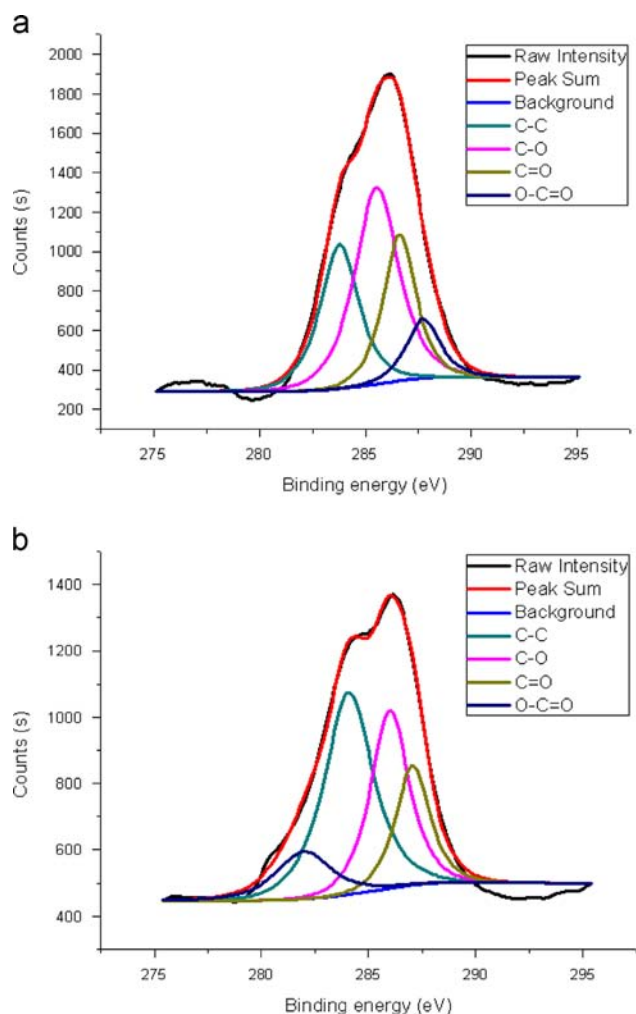


Fig. 3. The C 1s XPS spectra of GO (a) and GO-silica composite (b).

three metal ions did not occur in the whole tested pH range. These results demonstrated that GO in the GO-silica composite coating mainly contributed to the adsorption of metal ions. The adsorption mechanism of the target metal ions on the GO-silica composite coating could be attributed to the chelation of the functional groups of GO including hydroxyl, epoxide, carboxyl and carbonyl groups with target metal ions. The silica in GO-silica composite coating mainly contributed to the coating stability. Finally, a sample pH of 5.0 was selected to guarantee quantitative adsorption of all target metal ions for further experiments.

### 3.3. Effect of the length of hollow fiber

The effect of the length of hollow fiber on the adsorption of target metal ions was studied with passing 1 mL sample solution (pH 5.0) containing target metal ion each at  $1 \mu\text{g L}^{-1}$  at the sample flow rate of  $0.2 \text{ mL min}^{-1}$  through the GO-silica composite coated hollow fiber. It was found that the recoveries of the studied metal ions were increased with the increase of the length of HF from 5 to 15 cm and quantitative recoveries were obtained when the length of HF was in the ranges of 15–20 cm. However, the dead volume and analytical time for one run will increase with the increase of the length of hollow fiber. To ensure the quantitative adsorption, minimize the dead volume and improve the analytical efficiency, the hollow fiber length of 15 cm was employed in this work.

### 3.4. Effect of $\text{HNO}_3$ concentration

It is clear in Fig. 5a that the adsorption percentages of target metal ions on GO-silica composite coated HF were sharply decreased with the decrease in pH value. Based on that,  $\text{HNO}_3$  was selected as the eluent and the effect of its concentration in the range of  $0.1\text{--}1.5 \text{ mol L}^{-1}$  on desorption of the retained target metal ions from the GO-silica composite coated HF was studied. The experimental results demonstrated that all target metal ions could be eluted quantitatively when the  $\text{HNO}_3$  concentration was in the range of  $0.1\text{--}1.5 \text{ mol L}^{-1}$ . In the following experiments,  $0.5 \text{ mol L}^{-1}$   $\text{HNO}_3$  was employed.

### 3.5. Effect of elution volume and flow rate

The elution volume and the elution flow rate could affect the efficiency of the elution significantly. To study the effect of elution volume on the desorption, five portions of  $50 \mu\text{L}$   $0.5 \text{ mol L}^{-1}$   $\text{HNO}_3$  were used as an eluent to sequentially elute the target metal ions retained on the GO-silica composite coated HF at a flow rate of  $50 \mu\text{L min}^{-1}$ . It was found that  $0.1 \text{ mL}$   $0.5 \text{ mol L}^{-1}$   $\text{HNO}_3$  was sufficient to elute quantitatively all the target metal ions. By using  $0.1 \text{ mL}$  of  $0.5 \text{ mol L}^{-1}$   $\text{HNO}_3$  as an eluent, the influence of elution flow rate varying from  $0.05$  to  $0.3 \text{ mL min}^{-1}$  on the recovery of the target metal ions was also investigated. The results indicated that the target metal ions could be recovered quantitatively when the elution flow rate was in the range of  $0.05\text{--}0.1 \text{ mL min}^{-1}$ . Finally,  $0.1 \text{ mL}$   $0.5 \text{ mol L}^{-1}$   $\text{HNO}_3$  with a flow rate of  $0.1 \text{ mL min}^{-1}$  was employed as the optimum elution conditions.

### 3.6. Effect of sample flow rate

The sample flow rate should be optimized to ensure quantitative retention along with the minimization of the time required for sample processing. To study the effect of sample flow rate,  $1 \text{ mL}$  of sample solution was passed through GO-silica composite coated HF with the flow rate varying from  $0.05$  to  $0.5 \text{ mL min}^{-1}$ . The experimental results indicated that quantitative recoveries could be obtained for the target metal ions at sample flow rates less than  $0.2 \text{ mL min}^{-1}$ . When the sample flow rate was beyond  $0.2 \text{ mL min}^{-1}$ , the recoveries for these target metal ions were decreased with the increase of the flow rate, due to a decrease in the adsorption kinetics at a high flow rate. Thus, a sample flow rate of  $0.2 \text{ mL min}^{-1}$  was employed in this work, and the carrier gas flow rate in ICP was optimized accordingly.

### 3.7. Effect of sample volume

In order to obtain a higher enrichment factor, a larger sample volume is required. The effect of the sample volume on the recoveries of the target metal ions was investigated by passing 1, 2, 5, 10, 12 and 15 mL of sample solutions containing 10 ng of each metal ion through the GO-silica composite coated HF under the above optimized conditions. It was found that quantitative recoveries for all target metal ions were obtained with sample volume ranging from 1 to 12 mL. Thus, an enrichment factor of 120 could be achieved (target metal ions were concentrated from 12 mL sample solution to 0.1 mL eluent). However, larger sample volume would take a longer time and thus resulting in a lower sampling frequency. To trade off enrichment factor and analytical speed,  $1 \text{ mL}$  sample solution and  $0.1 \text{ mL}$   $0.5 \text{ mol L}^{-1}$   $\text{HNO}_3$  as an eluent were selected in this work. Therefore, an enrichment factor of 10 was obtained with a sampling frequency of  $8 \text{ h}^{-1}$ .

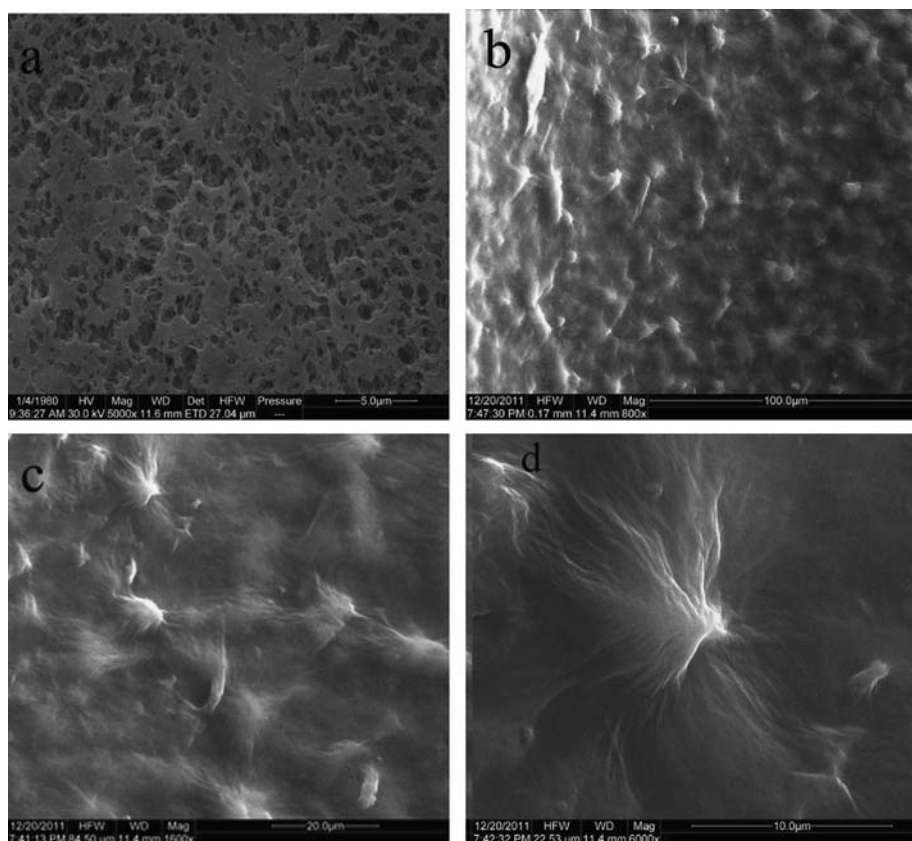


**Fig. 4.** SEM images of hollow fiber and GO-silica composite coated hollow fiber. Textural image of inner surface of hollow fiber (a); and GO-silica composite coated hollow fiber at magnifications of 800-folds (b); 1600-folds (c); 6000-folds (d).

### 3.8. Effect of coexisting ions

To study the effect of coexisting ions such as  $K^+$ ,  $Na^+$ ,  $Ca^{2+}$ ,  $Mg^{2+}$ ,  $Fe^{3+}$ ,  $Zn^{2+}$ ,  $Al^{3+}$  and  $Cr^{3+}$  on the extraction and determination of target metal ions, 1 mL sample solutions containing  $10 \mu\text{g L}^{-1}$  of each target metal ion and a certain amount of interfering ions were subjected to the proposed procedure. The tolerance limit was defined as the largest amount of coexisting ions with which the recovery of the target metal ions could be maintained in the range of 85–115%. The results show that  $1000 \text{ mg L}^{-1}$  (100,000-fold)  $K^+$ ,  $Na^+$ ,  $80 \text{ mg L}^{-1}$  (8000-fold)  $Ca^{2+}$ ,  $100 \text{ mg L}^{-1}$  (10,000-fold)  $Mg^{2+}$ ,  $10 \text{ mg L}^{-1}$  (1000-fold)  $Fe^{3+}$ ,  $Zn^{2+}$ ,  $5 \text{ mg L}^{-1}$  (500-fold)  $Cr^{3+}$ ,  $1 \text{ mg L}^{-1}$  (100-fold)  $Al^{3+}$ ,  $1500 \text{ mg L}^{-1}$  (150,000-fold)  $Cl^-$  and  $NO_3^-$  or  $800 \text{ mg L}^{-1}$  (80,000-fold)  $SO_4^{2-}$  had no significant effect on the extraction and determination of target metal ions. Therefore, it can be concluded that the GO-silica composite coating has an excellent selectivity for the adsorption of Mn, Co, Ni, Cu, Cd and Pb under the selected conditions.

The possible polyatomic interference for ICP-MS determination of Mn, Co, Ni, Cu, Cd and Pb was also investigated in this study. According to the Agilent 7500a ICP-MS operator's manual, tuning solution containing  $10 \text{ ng mL}^{-1}$  Li, Y, Ba, Ce and Tl was used to optimize instrument conditions to achieve good sensitivity and reduce the production oxide ions and doubly charged ions. The criteria for the optimization is as follows: the counts/ $10 \mu\text{g L}^{-1}$  (integrate time of 0.1 s) for  $^7\text{Li}$ ,  $^{89}\text{Y}$ , and  $^{205}\text{Tl}$  are higher than 20,000, and the ratio of oxide mass ( $^{140}\text{Ce}^{16}\text{O}^+$ ) to the element mass ( $^{140}\text{Ce}^+$ ) and the ratio of the signal of the doubly charged ion ( $^{137}\text{Ba}^{2+}$ ) to the element ( $^{137}\text{Ba}^+$ ) signal are lower than 1% and 3%, respectively. Besides, the developed GO-silica composite coated HF-SPME has good cleanup ability since the coexisting ions such as

$K^+$ ,  $Na^+$ ,  $Ca^{2+}$ ,  $Mg^{2+}$ ,  $NO_3^-$ ,  $SO_4^{2-}$  and  $Cl^-$  could be tolerated at high concentration. At their tolerant limits of the coexisting ions, the polyatomic interference of  $^{40}\text{Ar}^{14}\text{N}^{1}\text{H}$ ,  $^{39}\text{K}^{16}\text{O}$ ,  $^{37}\text{Cl}^{18}\text{O}$ ,  $^{40}\text{Ar}^{15}\text{N}$  and  $^{23}\text{Na}^{32}\text{S}$  on  $^{55}\text{Mn}$ ;  $^{43}\text{Ca}^{16}\text{O}$ ,  $^{24}\text{Mg}^{35}\text{Cl}$  and  $^{36}\text{Ar}^{23}\text{Na}$  on  $^{59}\text{Co}$ ;  $^{44}\text{Ca}^{16}\text{O}$ ,  $^{23}\text{Na}^{37}\text{Cl}$  and  $^{43}\text{Ca}^{16}\text{O}^{1}\text{H}$  on  $^{60}\text{Ni}$ ;  $^{40}\text{Ar}^{23}\text{Na}$ ,  $^{47}\text{Ti}^{16}\text{O}$ ,  $^{23}\text{Na}^{40}\text{Ca}$ ,  $^{46}\text{Ca}^{16}\text{O}^{1}\text{H}$  on  $^{63}\text{Cu}$  were found to be negligible. The polyatomic interference of  $^{40}\text{Ar}^{18}\text{O}$  and  $^{58}\text{Fe}$  on  $^{58}\text{Ni}$  could also be avoided by the selection of nickel isotopes at  $m/z$  60. The Mo, Nb, Os, Ir and Pt in analyzed environmental water samples are at a low level. So the polyatomic interference of  $^{95}\text{Mo}^{16}\text{O}$  and  $^{93}\text{Nb}^{18}\text{O}$  on  $^{111}\text{Cd}$ ,  $^{16}\text{O}^{192}\text{Os}$ ,  $^{17}\text{OH}^{191}\text{Ir}$  and  $^{14}\text{N}^{194}\text{Pt}$  on  $^{208}\text{Pb}$  could also be ignored.

### 3.9. Adsorption capacity

Adsorption capacity is one of the key factors for evaluating the performance of the adsorption coating. The method used in adsorption capacity study was adapted from the procedure that was recommended by Hu et al. [5]. To evaluate the adsorption capacity of the prepared GO-silica composite coating, 70 mL sample solution containing  $50 \mu\text{g L}^{-1}$  of each target metal ion was passed through the GO-silica composite coated HF (15 cm) and the analytes in the effluent were determined by ICP-MS. The maximal adsorption capacities evaluated from the breakthrough curve as mass amount of adsorbed analytes ( $\mu\text{g}$ ) per meter of GO-silica composite coated HF (m) were 4.6, 5.5, 7.4, 5.6, 16 and  $25 \mu\text{g m}^{-1}$  for Mn, Co, Ni, Cu, Cd and Pb, respectively. For comparison, the adsorption capacity of GO-silica composite coating and the other coating materials in in-tube SPME for the determination of trace metals are listed in Table 2. As can be seen, the adsorption capacity of GO-silica composite coating is higher than that obtained by other reported coating materials. Although

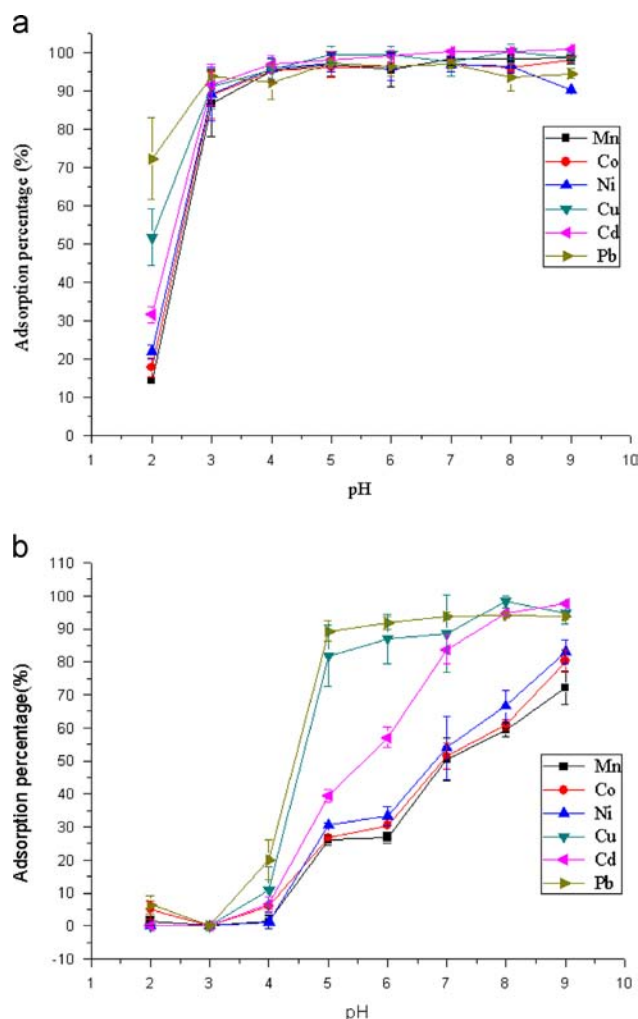


**Fig. 5.** Effect of pH on the adsorption percentage of  $\text{Mn}^{2+}$ ,  $\text{Co}^{2+}$ ,  $\text{Ni}^{2+}$ ,  $\text{Cu}^{2+}$ ,  $\text{Cd}^{2+}$  and  $\text{Pb}^{2+}$  on the GO-silica composite coated hollow fiber (a) and silica coated hollow fiber (b); sample volume: 1 mL; sample flow rate:  $50 \mu\text{L min}^{-1}$ ; concentration of each target metal ion:  $1 \mu\text{g L}^{-1}$ .

**Table 2**  
Comparison of adsorption capacities ( $\mu\text{g m}^{-1}$ ).

Coating	Mn	Co	Ni	Cu	Cd	Pb	Ref.
$\text{Al}_2\text{O}_3$	–	0.83	1.19	–	1.90	–	5
MPTS-silica	–	–	–	1.17	–	1.19	9
APTES-silica monolith	42.5	55	57.5	82.5	52.5	40	42
AAPTS-silica	–	–	2.84	3.43	1.64	–	43
GO-silica composite	4.6	5.5	7.4	5.6	16	25	This work

the adsorption capacity of GO-silica composite coating was lower than that obtained by APTES-silica monolithic capillary, its adsorption kinetics was faster than the latter.

### 3.10. Reproducibility and lifetime of the prepared GO-silica composite coated hollow fiber

In order to evaluate the preparation reproducibility of GO-silica composite coated HF, the extraction efficiencies of five segments of GO-silica composite coated HF prepared in the same batch and among different batches were investigated under the optimum conditions. As shown in Table 3, the relative standard deviations (RSDs) were in the range of 6.8–10.1% ( $c_{\text{Mn, Co, Cd}}=0.05 \mu\text{g L}^{-1}$ ,  $c_{\text{Ni, Cu, Pb}}=0.2 \mu\text{g L}^{-1}$ ) and 1.5–5.6% ( $c=10 \mu\text{g L}^{-1}$ ) within one batch

**Table 3**  
Preparation reproducibility for GO-silica composite coated hollow fiber.

Elements	One batch		Batch to batch	
	RSD (%) <sup>a</sup>	RSD (%) <sup>b</sup>	RSD (%) <sup>a</sup>	RSD (%) <sup>b</sup>
Mn	6.8	2.4	10.9	3.4
Co	10.1	1.5	11.9	2.9
Ni	8.6	3.6	13.4	7.6
Cu	9.6	5.6	15.1	4.2
Cd	9.3	2.6	12.7	3.1
Pb	7.8	3.4	12.1	2.7

<sup>a</sup>  $c_{\text{Mn, Co, Cd}}=0.05 \mu\text{g L}^{-1}$ ,  $c_{\text{Ni, Cu, Pb}}=0.2 \mu\text{g L}^{-1}$ .

<sup>b</sup>  $c=10 \mu\text{g L}^{-1}$  ( $n=5$ ).

as well as 10.9–15.1% ( $c_{\text{Mn, Co, Cd}}=0.05 \mu\text{g L}^{-1}$ ,  $c_{\text{Ni, Cu, Pb}}=0.2 \mu\text{g L}^{-1}$ ) and 2.7–7.6% ( $c=10 \mu\text{g L}^{-1}$ ) from batch to batch. These results indicated that the preparation of GO-silica composite coated HF possessed a good reproducibility. The lifetime of GO-silica composite coated HF was also studied, and it was found that the GO-silica composite coated HF could be reused for more than 50 times without decrease of the extraction performance for the target metal ions under the optimum conditions.

### 3.11. Analytical performance

Under the optimum conditions, an enrichment factor of 10-fold and a sampling frequency of  $8 \text{ h}^{-1}$  with a preconcentration time of 300 s and an elution time of 60 s were obtained by HF-SPME for the target metal ions. The analytical performance of on-line GO-silica composite coated HF-SPME-ICP-MS is summarized in Table 4. According to the IUPAC definition, the limits of detection (LODs,  $3\sigma$ ) of the method, defined as three times the standard deviation of blank signal intensity, were 7.5, 0.39, 20, 23, 6.7 and  $28 \text{ ng L}^{-1}$  for Mn, Co, Ni, Cu, Cd and Pb, respectively. The RSDs for seven replicate determinations of  $1 \mu\text{g L}^{-1}$  of the target metals were in the range of 4.6–7.8% ( $c_{\text{Mn, Co, Cd}}=0.05 \mu\text{g L}^{-1}$ ,  $c_{\text{Ni, Cu, Pb}}=0.2 \mu\text{g L}^{-1}$ ) and 1.2–5.1% ( $c=1 \mu\text{g L}^{-1}$ ), respectively. For comparison, the LODs of the proposed method with that obtained by other approaches are listed in Table 5. As can be seen, the LODs obtained by this work were lower than that reported in Refs. [43,44], and comparable with that reported in Refs. [45,46], but higher than that reported in Refs. [42,47]. However, the developed method is an on-line analytical method based on the fast adsorption/desorption kinetics of the prepared GO-silica composite, and consumes much less sample/reagents, which are the obvious advantages over other similar methods mentioned above [43–47].

### 3.12. Sample analysis

In order to establish the validity of the proposed method, the method has been applied to the determination of trace Mn, Co, Ni, Cu, Cd and Pb in Certified Reference Materials of GSBZ 50009-88 environmental water for five replicates, and the Student *t*-test was performed. The analytical results listed in Table 6 indicated that the determined values were in good agreement with the certified values.

The proposed method was also applied to the determination of target metal ions in environmental water samples (lake, well and pond water). The analytical results and the recoveries for the spiked samples are given in Table 7. It can be seen that the recoveries for the spiked samples were between 85% and 119%.

**Table 4**  
The analytical performance data of the on-line HF-SPME-ICP-MS system.

Metal ions	Linear equation	$R^2$	Linear range ( $\mu\text{g L}^{-1}$ )	LOD ( $\text{ng L}^{-1}$ )	RSD (%)	
					a	b
Mn	$y=1,220,110x+295,433$	0.999	0.03–50	7.5	7.5	2.2
Co	$y=1,231,710x-18,544$	0.999	0.01–50	0.39	7.0	1.2
Ni	$y=234,336x+31,329$	0.999	0.1–50	20	5.6	2.4
Cu	$y=374,312x+208,675$	0.997	0.1–50	23	7.3	5.1
Cd	$y=131,230x-6533$	0.999	0.03–50	6.7	7.8	3.2
Pb	$y=563,598x+323,376$	0.994	0.1–50	28	4.6	3.7

<sup>a</sup>  $C_{\text{Mn, Co, Cd}}=0.05 \mu\text{g L}^{-1}$ ,  $C_{\text{Ni, Cu, Pb}}=0.2 \mu\text{g L}^{-1}$ .

<sup>b</sup>  $c=1 \mu\text{g L}^{-1}$  ( $n=7$ ).

**Table 5**  
Comparison of limits of detection ( $\text{ng L}^{-1}$ ) for  $\text{Mn}^{2+}$ ,  $\text{Co}^{2+}$ ,  $\text{Ni}^{2+}$ ,  $\text{Cu}^{2+}$ ,  $\text{Cd}^{2+}$  and  $\text{Pb}^{2+}$  obtained by the proposed method with other analytical approaches.

Sorbents/coating	Methods	Mn	Co	Ni	Cu	Cd	Pb	Ref.
APTES-silica	CME-ICP-MS	6.2	1.5	5.2	6.3	1.2	14	42
Polymer	SPE-ICP-MS	–	5.84	–	–	–	–	43
MNPs-PAA <sup>a</sup>	On-line SPE-ICP-MS	60	40	–	600	–	60	44
SWNTs <sup>b</sup>	SPE-ICP-MS	–	1.2	–	39	–	5.4	45
Polymer	On-line SPE-ICP-MS	–	–	35	31	5	5	46
$\text{Fe}_3\text{O}_4@/\text{SiO}_2@/\text{TiO}_2$	SPE-ICP-MS	1.6	–	–	2.3	4	–	47
GO-silica composite	On-line HF-SPME-ICP-MS	7.5	0.39	20	23	6.7	28	This work

<sup>a</sup> MNPs-PAA, iron-based magnetic nanoparticles with polyacrylic acid.

<sup>b</sup> SWNTs, single-walled carbon nanotubes

**Table 6**

Analytical results of Mn, Co, Ni, Cu, Cd and Pb in certified reference material of GSBZ50009-88 environmental water (mean  $\pm$  s.d.,  $n=5$ ).

Elements	Certified ( $\text{mg L}^{-1}$ )	Determined ( $\text{mg L}^{-1}$ )	$t$ -test <sup>b</sup>
Mn	–	N.D. <sup>a</sup>	–
Co	–	N.D.	–
Cd	$0.113 \pm 0.005$	$0.115 \pm 0.002$	2.24
Pb	$1.21 \pm 0.05$	$1.23 \pm 0.04$	1.12
Ni	$0.599 \pm 0.027$	$0.602 \pm 0.050$	0.13
Cu	$1.10 \pm 0.04$	$1.18 \pm 0.07$	2.56

<sup>a</sup> N.D., not detected.

<sup>b</sup>  $t_{0.05,4}=2.78$ .

**Table 7**  
Analytical results of Mn, Co, Ni, Cu, Cd and Pb in environmental water samples (mean  $\pm$  s.d.,  $n=3$ ).

Samples	East lake water ( $\mu\text{g L}^{-1}$ )		Well water ( $\mu\text{g L}^{-1}$ )		Pond water ( $\mu\text{g L}^{-1}$ )	
Mn						
Added	0	5.0	0	1.0	0	1.0
Found	$4.6 \pm 0.3$	$10.0 \pm 0.5$	$1.00 \pm 0.04$	$1.9 \pm 0.1$	$1.40 \pm 0.04$	$2.30 \pm 0.01$
Recovery %	–	107	–	88	–	85
Co						
Added	0	1.0	0	1.0	0	1.0
Found	$0.13 \pm 0.01$	$1.10 \pm 0.03$	N.D. <sup>a</sup>	$0.88 \pm 0.05$	$0.030 \pm 0.001$	$0.95 \pm 0.03$
Recovery %	–	93	–	88	–	92
Ni						
Added	0	5.0	0	5.0	0	5.0
Found	$1.6 \pm 0.2$	$6.2 \pm 0.1$	$7.5 \pm 0.1$	$11.9 \pm 0.3$	$2.20 \pm 0.02$	$6.8 \pm 0.2$
Recovery %	–	92	–	90	–	91
Cu						
Added	0	1.0	0	1.0	0	5.0
Found	$2.7 \pm 0.1$	$3.8 \pm 0.3$	$3.3 \pm 0.2$	$4.20 \pm 0.03$	$6.7 \pm 0.3$	$11.2 \pm 0.2$
Recovery %	–	112	–	97	–	91
Cd						
Added	0	1.0	0	1.0	0	1.0
Found	$0.100 \pm 0.005$	$1.10 \pm 0.02$	$0.230 \pm 0.004$	$1.2 \pm 0.1$	$0.150 \pm 0.003$	$1.20 \pm 0.03$
Recovery %	–	107	–	100	–	101
Pb						
Added	0	1.0	0	1.0	0	1.0
Found	$1.80 \pm 0.04$	$3.0 \pm 0.2$	$1.2 \pm 0.1$	$2.1 \pm 0.1$	$4.0 \pm 0.2$	$4.90 \pm 0.05$
Recovery %	–	119	–	88	–	87

<sup>a</sup> N.D., not detected.



#### 4. Conclusions

In this paper, a novel graphene oxide–silica composite coated hollow fiber was prepared and applied to on-line hollow fiber solid phase microextraction (HF-SPME)–ICP-MS determination of trace metals in environmental waters. The prepared GO–silica composite coating possesses a high adsorption capacity, good preparation reproducibility, excellent chemical and mechanical stability as well as long lifespan (more than 50 extractions), and has a great potential as an adsorbent for the preconcentration of trace metal ions in real-world water samples.

#### Acknowledgments

The author would like to thank the National Basic Research Program of China (973 Program, 2013CB933900), the National Science Foundation of China (Nos. 20975076 and 21175102), and Science Fund for Creative Research Groups of NSFC (Nos. 20621502 and 20921062) for their financial supports. This work is also supported by “the Fundamental Research Funds for the Central Universities (114009)”.

#### References

- [1] M. Mehdizadeh, F. Kermandian, G. Farjah, *Pathophysiology* 15 (2008) 13–17.
- [2] N. Coen, C. Mothersill, M. Kadhim, E.G. Wright, *J. Pathol.* 195 (2001) 293–299.
- [3] L. Yang, R.E. Sturgeon, D. Prince, S. Gabos, *J. Anal. At. Spectrom.* 17 (2002) 1300–1303.
- [4] E. McCurdy, G. Woods, *J. Anal. At. Spectrom.* 19 (2004) 607–615.
- [5] W.L. Hu, B. Hu, Z.C. Jiang, *Anal. Chim. Acta* 572 (2006) 55–62.
- [6] L.B. Xia, B. Hu, Z.C. Jiang, Y.L. Wu, Y. Liang, *Anal. Chem.* 76 (2004) 2910–2915.
- [7] X.Q. Guo, M. He, B.B. Chen, B. Hu, *Talanta* 94 (2012) 70–76.
- [8] N. Zhang, B. Hu, *Anal. Chim. Acta* 723 (2012) 54–60.
- [9] F. Zheng, B. Hu, *Talanta* 73 (2007) 372–379.
- [10] A. Kabir, C. Hamlet, K.S. Yoo, G.R. Newkome, A. Malik, *J. Chromatogr. A* 1034 (2004) 1–11.
- [11] Y. Fan, Y.Q. Feng, S.L. Da, Z.G. Shi, *Anal. Chim. Acta* 523 (2004) 251–258.
- [12] J.J. Chen, Y.C. Lee, H.C. Lin, R.L.C. Chen, *J. Food Drug Anal.* 12 (2004) 332–335.
- [13] Z. Mester, J. Pawliszyn, *Rapid Commun. Mass Spectrom.* 13 (1999) 1999–2003.
- [14] C. Bicchi, C. Cordero, E. Liberto, B. Sgorbini, P. Rubiolo, *J. Chromatogr. A* 1184 (2008) 220–233.
- [15] J.C. Wu, Z. Mester, J. Pawliszyn, *Anal. Chim. Acta* 424 (2000) 211–222.
- [16] R. Kuldvee, S.K. Wiedmer, K. Öörni, M.L. Riekkola, *Anal. Chem.* 77 (2005) 3401–3405.
- [17] L.M. Yuan, C.X. Ren, L. Li, P. Ai, Z.H. Yan, M. Zi, Z.Y. Li, *Anal. Chem.* 78 (2006) 6384–6390.
- [18] X.J. Huang, Q.Q. Wang, B.L. Huang, *Talanta* 69 (2006) 463–468.
- [19] B.B. Chen, B. Hu, M. He, X.J. Mao, W.Q. Zu, *J. Chromatogr. A* 1227 (2012) 19–28.
- [20] C. Basheer, V. Suresh, R. Renu, H.K. Lee, *J. Chromatogr. A* 1033 (2004) 213–220.
- [21] K.S. Novoselov, A.K. Geim, S.V. Morozov, D. Jiang, Y. Zhang, S.V. Dubonos, I.V. Grigorieva, A.A. Firsov, *Science* 306 (2004) 666–669.
- [22] A.K. Geim, K.S. Novoselov, *Nat. Mater.* 6 (2007) 183–191.
- [23] M.D. Stoller, S.J. Park, Y.W. Zhu, J.H. An, R.S. Ruoff, *Nano Lett.* 8 (2008) 3498–3502.
- [24] C. Lee, X.D. Wei, J.W. Kysar, J. Hone, *Science* 321 (2008) 385–388.
- [25] K.I. Bolotin, K.J. Sikes, Z. Jiang, M. Klima, G. Fudenberg, J. Hone, P. Kim, H.L. Stormer, *Solid State Commun.* 146 (2008) 351–355.
- [26] Y. Cai, G. Jiang, J. Liu, Q. Zhou, *Anal. Chem.* 75 (2003) 2517–2521.
- [27] Q. Liu, J.B. Shi, L.X. Zeng, T. Wang, Y.Q. Cai, G.B. Jiang, *J. Chromatogr. A* 1218 (2011) 197–204.
- [28] J.M. Chen, J. Zou, J.B. Zeng, X.H. Song, J.J. Ji, Y.R. Wang, J. Ha, X. Chen, *Anal. Chim. Acta* 678 (2010) 44–49.
- [29] H. Zhang, H.K. Lee, *J. Chromatogr. A* 1218 (2011) 4509–4516.
- [30] S. Zhang, Z. Du, G. Li, *Anal. Chem.* 83 (2011) 7531–7541.
- [31] V.K. Ponnusamy, J.F. Jen, *J. Chromatogr. A* 1218 (2011) 6861–6868.
- [32] X. Deng, L. Lü, H. Li, F. Luo, *J. Hazard. Mater.* 183 (2010) 923–930.
- [33] V. Chandra, K.S. Kim, *Chem. Commun.* 47 (2011) 3942–3944.
- [34] D.W. Boukhvalov, M.I. Katsnelson, *J. Am. Chem. Soc.* 130 (2008) 10697–10701.
- [35] K.N. Kudin, B. Ozbas, H.C. Schniepp, R.K. Prud'homme, I.A. Aksay, R. Car, *Nano Lett.* 8 (2008) 36–41.
- [36] S.T. Yang, Y.L. Chang, H.F. Wang, G.B. Liu, S. Chen, Y.W. Wang, Y.F. Liu, A.N. Cao, *J. Colloid Interf. Sci* 351 (2010) 122–127.
- [37] G. Zhao, X. Ren, X. Gao, X. Tan, J. Li, C. Chen, Y. Huang, X. Wang, *Dalton Trans.* 40 (2011) 10945–10952.
- [38] W.S. Hummers, R.E. Offeman, *J. Am. Chem. Soc.* 80 (1958) 1339 (1339).
- [39] N.I. Kovtyukhova, P.J. Ollivier, B.R. Martin, T.E. Mallouk, S.A. Chizhik, E.V. Buzaneva, A.D. Gorchinskiy, *Chem. Mater.* 11 (1999) 771–778.
- [40] G.I. Titelman, V. Gelman, S. Bron, R.L. Khalfin, Y. Cohen, H. Bianco-Peled, *Carbon* 43 (2005) 641–649.
- [41] S. Stankovich, D.A. Dikin, R.D. Piner, K.A. Kohlhaas, A. Kleinhammes, Y. Jia, Y. Wu, S.T. Nguyen, R.S. Ruoff, *Carbon* 45 (2007) 1558–1565.
- [42] L. Zhang, B.B. Chen, H.Y. Peng, M. He, B. Hu, *J. Sep. Sci.* 34 (2011) 2247–2254.
- [43] X. Zhu, M. Wu, Y. Gu, *Talanta* 78 (2009) 565–569.
- [44] P.L. Lee, Y.C. Sun, Y.C. Ling, *J. Anal. At. Spectrom.* 24 (2009) 320–327.
- [45] S. Chen, C. Liu, M. Yang, D. Lu, L. Zhu, Z. Wang, *J. Hazard. Mater.* 170 (2009) 247–251.
- [46] T.T. Shih, W.Y. Tseng, K.H. Tsai, W.Y. Chen, M.W. Tsai, Y.C. Sun, *Microchem. J.* 99 (2011) 260–266.
- [47] N. Zhang, H.Y. Peng, B. Hu, *Talanta* 94 (2012) 278–283.